Superimposed Effects of Brill Waves and Scalar Fields in Axisymmetric Critical Collapse

Sylvia Mesicek[1], Sean Johnson[1], Benjamin Derieg[1], John Belz[1]

[1]Department of Physics and Astronomy, University of Utah | Salt Lake City, Utah

Introduction

In the parameter space near the threshold of black hole formation (given an arbitrary initial system of mass and energy) numerical analysis reveals an intriguing degree of structure to resulting spacetimes. Drawing analogy to phase transitions in thermodynamics, Choptuik's pioneering work observed three kinds of "critical phenomena" in this regime [1].

- Power-law mass scaling: $M \propto |p - p^*|^\gamma$
- Universality: the resulting solution and critical exponent γ is independent of the profile of initial data
- The solution repeats itself on increasingly small spatio-temporal scales (echoing)

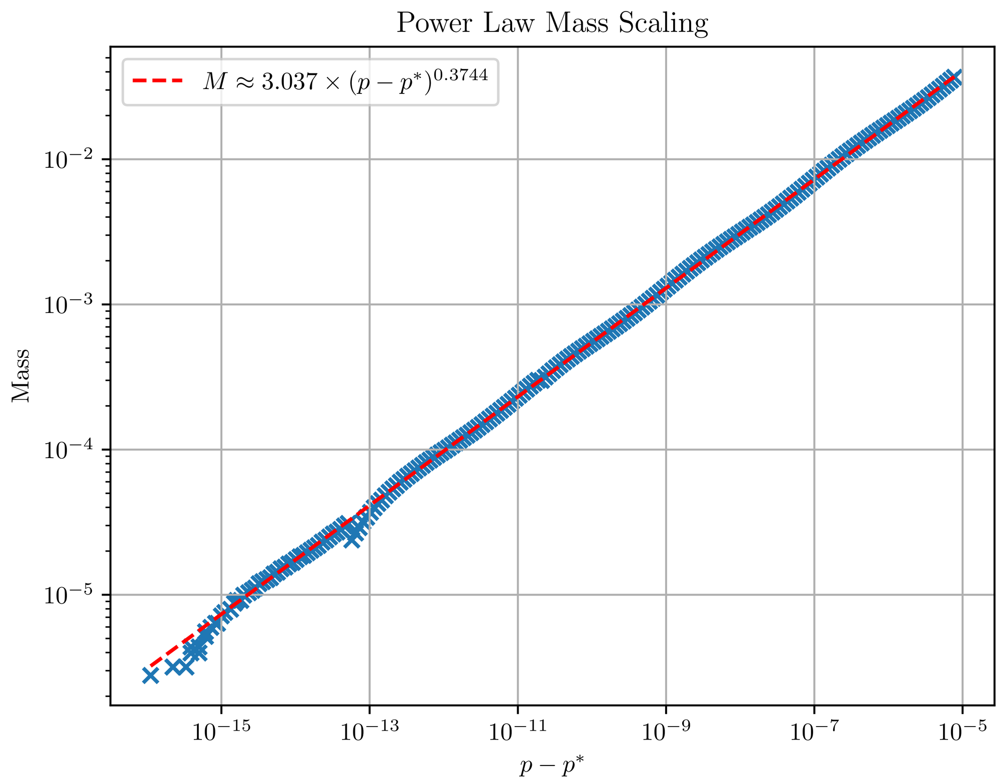

Figure 1: Power law mass scaling of a scalar field with profile $\Phi = p\exp(-r^2/5.35^2)$ in spherical symmetry.

These solutions have proven to be a powerful test of cosmic censorship. However, they are less understood in higher dimensional systems, which pose computational challenges and incorporate additional physical effects such as gravitational waves [2].

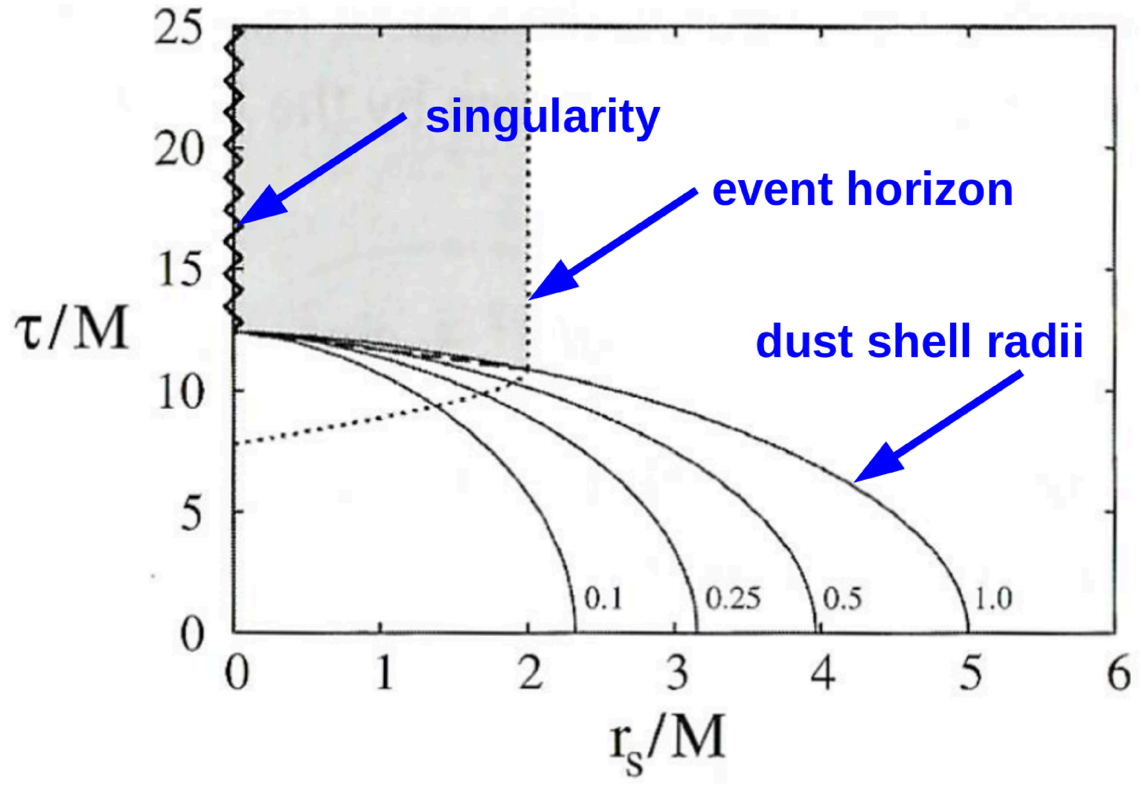

Figure 2: Example of cosmic censorship in the case of dust collapse. For typical initial data, an event horizon will always form in a region before a curvature singularity does [3].

Mathematical Formulation

- The Einstein field equations are transformed into strongly hyperbolic form using the Z4 extension
$$R_{ab} - \frac{1}{2}Rg_{ab} + 2\nabla_{(a}Z_{b)} = \kappa T_{ab}$$
- We introduce a global time coordinate using the ADM decomposition [3]
- Axisymmetry is enforced via the Geroch decomposition [4]

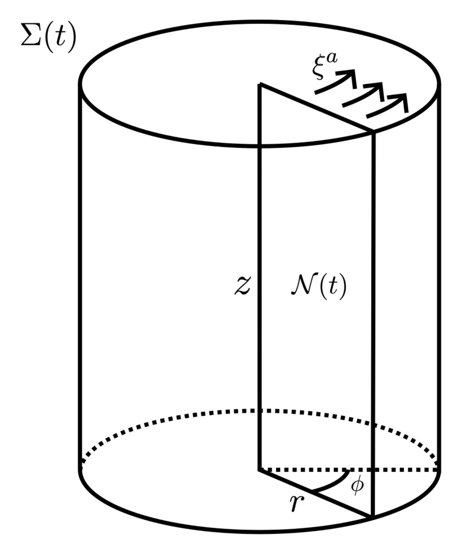

Figure 3: Spatial tensors can be decomposed into components either orthogonal or parallel to $\xi^a = \partial/\partial\phi$.

Hamiltonian Constraint:

$$\frac{1}{2}(X^2 - X_{AB}X^{AB} + \mathcal{R}) - \frac{D_A D^A \lambda}{\lambda} + XL = 0$$

Evolution Equations:

$$\mathcal{L}_n h_{AB} = -2X_{AB}, \ \mathcal{L}_n \lambda = -\lambda L$$

Final Decomposition:

$$g_{ab} = \begin{pmatrix} -\alpha^2 + \beta_A\beta^A & \beta_r & \beta_z & 0 \\ \beta_r & h_{rr} & h_{rz} & 0 \\ \beta_z & h_{zr} & h_{zz} & 0 \\ 0 & 0 & 0 & \lambda^2 \end{pmatrix}, K_{ij} = \begin{pmatrix} X_{rr} & X_{rz} & 0 \\ X_{zr} & X_{zz} & 0 \\ 0 & 0 & L \end{pmatrix}, Z_a = \begin{pmatrix} \Theta \\ \mathcal{Z}_r \\ \mathcal{Z}_z \\ 0 \end{pmatrix}$$

Prolate Scalar Fields

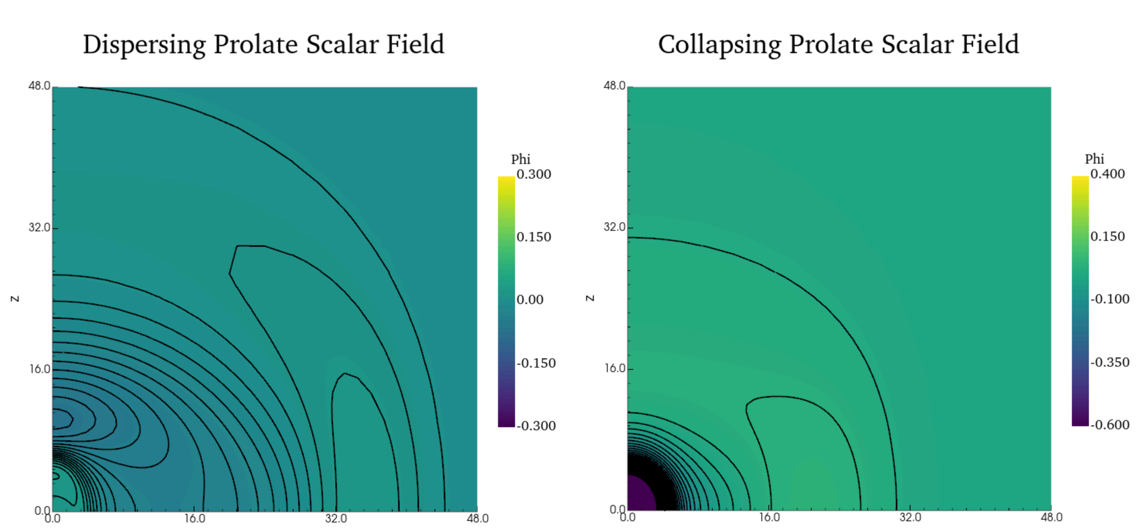

Figure 4: Dispersing (left) and collapsing (right) prolate scalar fields. The top displays a snapshot of each evolution while the bottom links to animations of each evolution.

Numerical Methods

- Spatial derivatives computed using the finite difference method
- Adaptive mesh refinement is performed via interpolating wavelets (inspired by Dendro GR [5])
- Temporal integration using 4th order Runge-Kutta method and 6th order Kreiss-Olgier Dissipation [6]
- Solve for initial data with hyperbolic relaxation [7], transforming the elliptic constraint equation
$$\mathcal{L}_E \boldsymbol{u} - \boldsymbol{p} = 0$$
into a hyperbolic equation by introducing a fictitious time variable and evolving to a steady-state
$$\partial_t^2 \boldsymbol{u} + \eta\partial_t \boldsymbol{u} = c^2(\mathcal{L}_E \boldsymbol{u} - \boldsymbol{p})$$

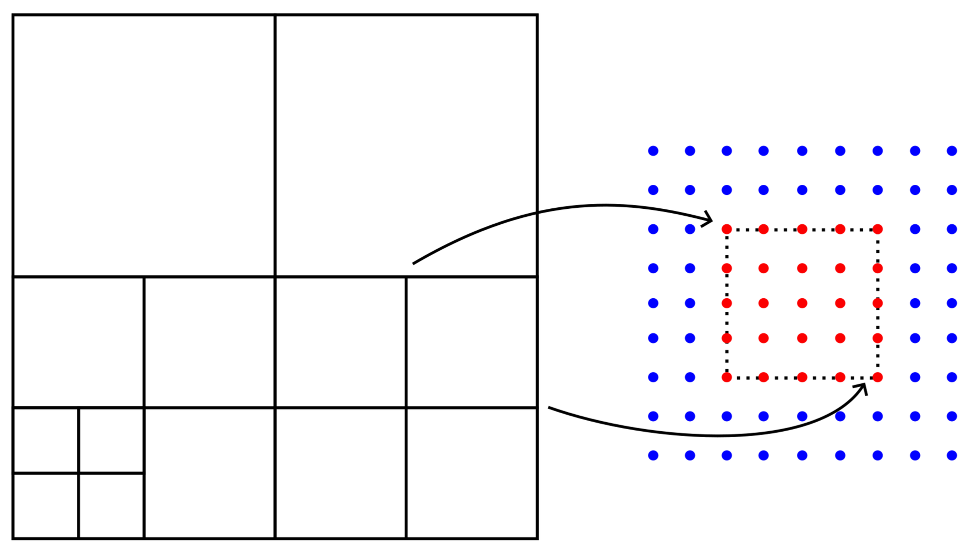

Figure 5: Domain is discretized by a quadtree of cells, each of which contains a uniform grid of physical nodes (red) padded by ghost nodes (blue).

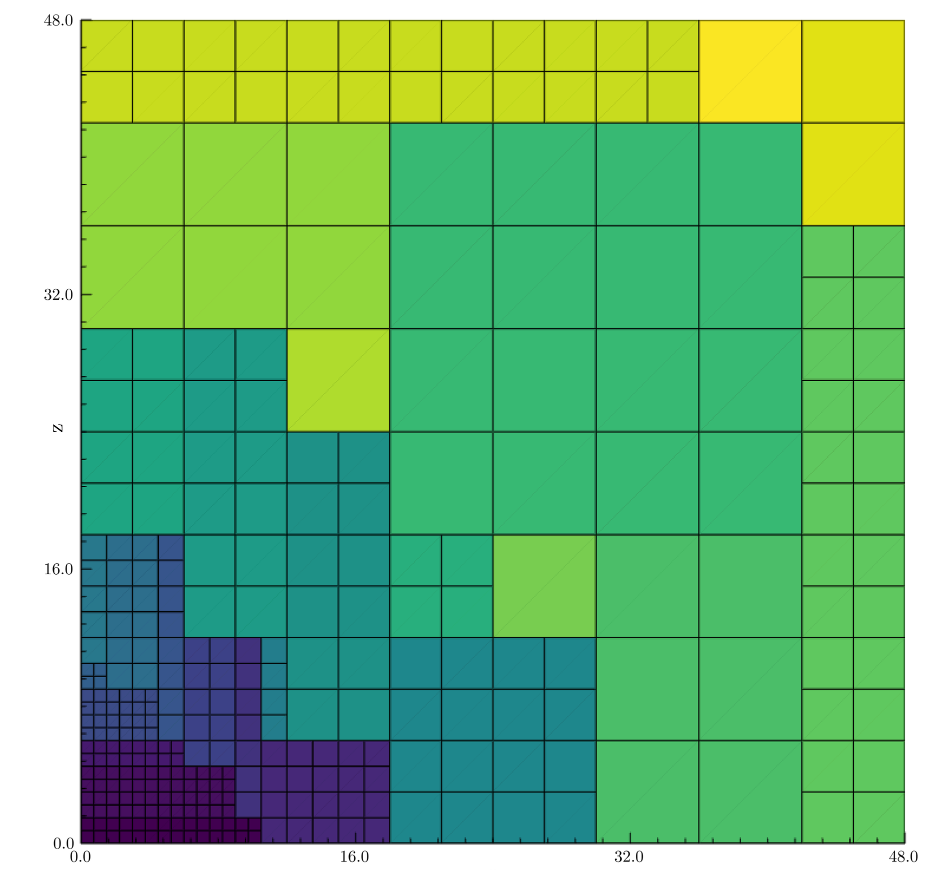

Figure 6: Adaptive mesh generated when solving initial data. Coloring indicates cells of the same level of refinement that have been grouped together for efficiency.

Acknowledgements

This project was funded in part by the University of Utah Physics & Astronomy Summer Undergraduate Research Fellowship (SURF) and the University of Utah Undergraduate Research Opportunity Program (UROP).

Office of Undergraduate Studies
UNDERGRADUATE RESEARCH
THE UNIVERSITY OF UTAH

Scalar Fields + Brill Waves

To understand the impact of higher dimensions on critical phenomena we simulated massless scalar field initial data with a superimposed nonlinear gravity wave known as a Brill wave. The addition of this wave reduces the critical point and dampens subsequent echos.

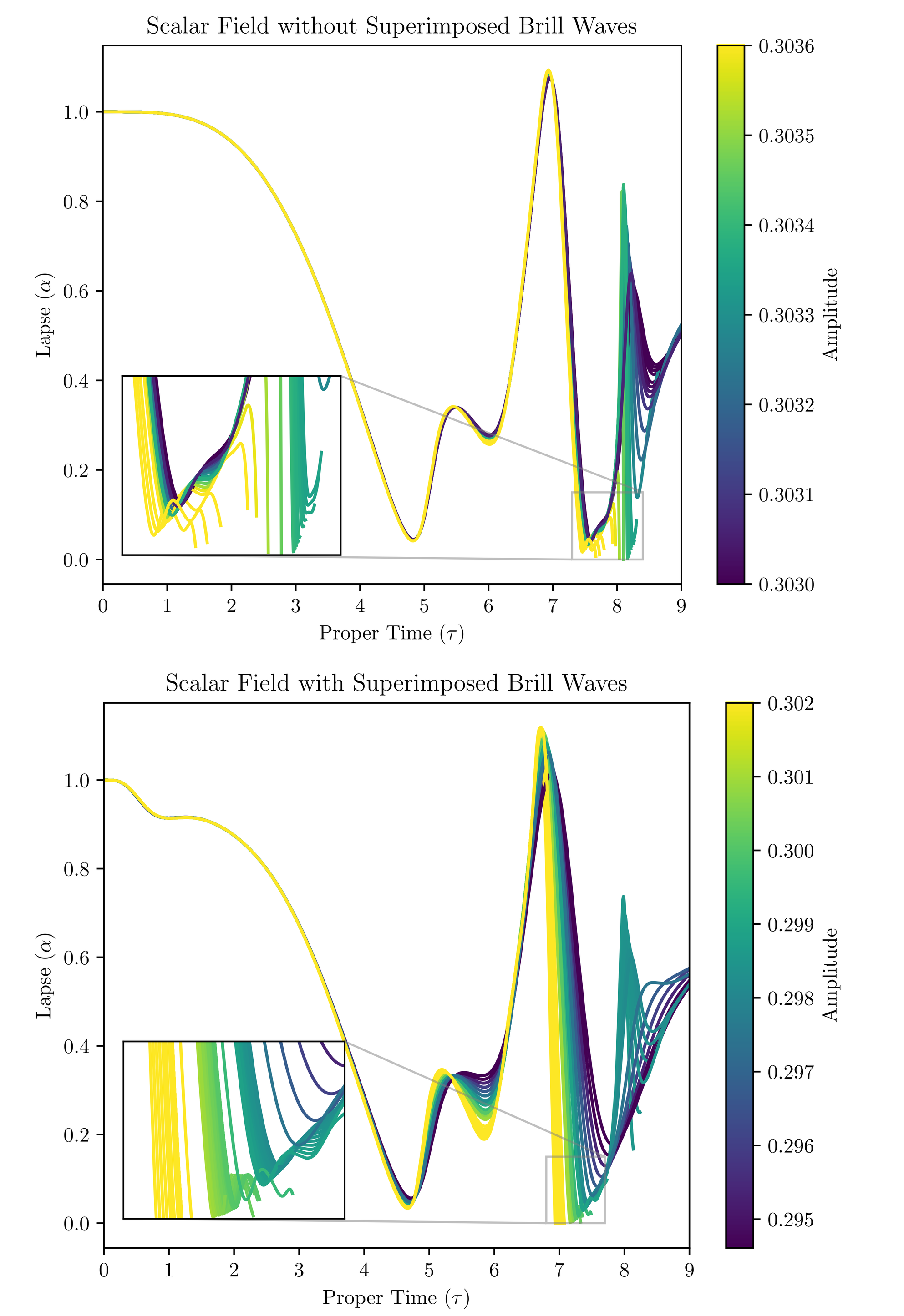

Figure 7: Lapse at the origin for a single scalar field (top) and a scalar field superimposed with a subcritical Brill wave (bottom).

Future Work

- Further resolve critical point for superimposed collapse
- Build a 2d mass estimator in order to estimate critical exponent and test universality
- Confirm second bifurcation in prolate collapse

Bibliography

[1] M. W. Choptuik, "Universality and scaling in gravitational collapse of a massless scalar field," *Physical Review Letters*, vol. 70, no. 1, pp. 9–12, 1993, doi: 10.1103/physrevlett.70.9.

[2] C. Gundlach, "Critical phenomena in gravitational collapse," *Encyclopedia of Mathematical Physics*, pp. 668–673, 2006, doi: 10.1016/b0-12-512666-2/00010-9.

[3] T. W. Baumgarte and S. L. Shapiro, *Numerical relativity: solving einstein's equations on the computer.* Cambridge University Press, 2010.

[4] O. Rinne, "Axisymmetric Numerical Relativity." 2013.

[5] M. Fernando, D. Neilsen, Y. Zlochower, E. W. Hirschmann, and H. Sundar, "Massively parallel simulations of binary black holes with adaptive wavelet multiresolution," *Physical Review D*, vol. 107, no. 6, 2023, doi: 10.1103/physrevd.107.064035.

[6] M. Alcubierre, *Introduction to 3+1 numerical relativity.* in International series of monographs on physics. Oxford: Oxford University Press, 2008. [Online]. Available: https://cds.cern.ch/record/1138167

[7] T. Assumpção, L. R. Werneck, T. Pierre Jacques, and Z. B. Etienne, "Fast hyperbolic relaxation elliptic solver for numerical relativity: Conformally flat, binary puncture initial data," *Physical Review D*, vol. 105, no. 10, 2022, doi: 10.1103/physrevd.105.104037.

Contact: sylvia.mesicek@utah.edu | sylviamesicek.github.io, belz@physics.utah.edu